

Improved algorithm for periodic steady-state analysis in nonlinear electromagnetic devices

T.J. SOB CZYK^{1*} and M. RADZIK²

¹Cracow University of Technology, Institute on Electromechanical Energy Conversion, 24 Warszawska St, 31-155 Cracow, Poland

²Technical Institute, State Higher Vocational School in Nowy Sącz, 1A Zamenhofska St., 33-300 Nowy Sącz, Poland

Abstract. This paper presents the improved methodology for the direct calculation of steady-state periodic solutions for electromagnetic devices, as described by nonlinear differential equations, in the time domain. A novel differential operator is developed for periodic functions and the iterative algorithm determining periodic steady-state solutions in a selected set of time instants is identified. Its application to steady-state analysis is verified by an elementary example. The modified algorithm reduces the complexity of steady-state analysis, particularly for electromagnetic devices described by high-dimensional nonlinear differential equations.

Key words: electromagnetic devices, steady-state analysis, periodic solutions, analysis in time domain, discrete differential operator, iterative algorithms.

1. Introduction

Direct steady-state calculations for electromagnetic devices are a subject of continued research in both the frequency and time domains. The nonlinearities embedded in the mathematical models of such objects cause the time-domain approach [1–7] preferable over the frequency-domain approach [8–13]. The most commonly used modelling approach is the finite-difference method, where the derivatives are substituted with discrete finite-difference operators spanning the values at adjacent time points. In order to identify the steady states of nonlinear electromagnetic devices in engineering applications, the equations are solved numerically until the transient component disappears and only steady-state components remain. However, such an approach may be inefficient owing to the high computational complexity, creation of unnecessary data and necessity of using very advanced hardware and software. Direct steady-state analysis methods have been developed to overcome these challenges.

The steady states of electromagnetic devices are usually periodic, and the respective difference equations are obtained by assuming that the values at the beginning of the period are related to those at the end. The difference equations of nonlinear systems are also nonlinear and can be solved by applying iterative procedures. However, the dimensionality of steady-state difference equations may be very high, especially at high dimensions of differential equations describing electromagnetic objects. In order to omit the high dimensionality problem, numerical integration of the differential equations can be combined with a boundary problem searching for proper initial

values at integrations, an example of which is the waveform relaxation method [14–16].

In [4] the first-order discrete differential operator was defined and used in [5, 6] and [7] to create the finite-difference steady-state equations for nonlinear differential equations with periodic steady-state solutions. This new type operator relates first-derivative values of a periodic function to values of that function in a set of time instants that are uniquely distributed over the period.

This paper presents an improved algorithm that allows for the direct calculation of periodic steady-state performance in electromagnetic devices described by nonlinear differential equations, with reduced computational complexity. The proposed algorithm is tested by means of steady-state analysis of an elementary circuit with a nonlinear coil.

2. Novel algorithm

The modified algorithm is based on the discrete differential operator \mathbf{D}' , described in details in [4–7]. The operator \mathbf{D}' fulfils, for periodic vector function

$$\mathbf{x}(t) = \mathbf{x}(t + T) = [x_1(t) \ x_2(t) \ \dots \ x_N(t)]^T$$

the relation

$$\mathbf{x}'_s = \mathbf{D}' \cdot \mathbf{x}_s \quad (1)$$

where:

$$\mathbf{x}'_s = [\mathbf{x}'_R \ \dots \ \mathbf{x}'_1 \ \mathbf{x}'_0 \ \mathbf{x}'_{-1} \ \dots \ \mathbf{x}'_{-R}]^T$$

is the vector of first-derivative values and

$$\mathbf{x}_s = [\mathbf{x}_R \ \dots \ \mathbf{x}_1 \ \mathbf{x}_0 \ \mathbf{x}_{-1} \ \dots \ \mathbf{x}_{-R}]^T$$

is the vector of function values itself.

*e-mail: pesobczy@cyf-kr.edu.pl

Manuscript submitted 2018-12-10, revised 2019-02-13, initially accepted for publication 2019-02-20, published in October 2019

Matrices $\mathbf{l}_{n,k}$ and $\mathbf{u}_{n,k}$ are diagonal with elements $l_{n,k}$ and $u_{n,k}$, which can be determined based on matrix \mathbf{D} with 1D matrices \mathbf{d}_n . Such a matrix has dimensions $(2R + 1) \times (2R + 1)$ and depends on the number 'R' of the highest harmonic taken into account, but does not depend on the dimension 'N' of the differential equation set (3), which may be arbitrarily high. A classical algorithm can be used for the decomposition of such a matrix \mathbf{D} into lower and upper triangular matrices. Finally, equation (6) can be written as

$$\mathbf{L} \cdot \mathbf{U} \cdot \mathbf{x}_s^{i+1} = \mathbf{f}_s(\mathbf{x}_s^i) + \mathbf{d}_0 \cdot \mathbf{x}_s^i, \quad (9)$$

where

$$\mathbf{x}_s = [\mathbf{x}_R \ \cdots \ \mathbf{x}_1 \ \mathbf{x}_0 \ \mathbf{x}_{-1} \ \cdots \ \mathbf{x}_{-R}]^T, \\ \mathbf{f}_s(\mathbf{x}_s) = [\mathbf{f}_R \ \cdots \ \mathbf{f}_1 \ \mathbf{f}_0 \ \mathbf{f}_{-1} \ \cdots \ \mathbf{f}_{-R}]^T.$$

Substituting

$$\mathbf{y}_s^{i+1} = \mathbf{U} \cdot \mathbf{x}_s^{i+1}, \quad (10)$$

where

$$\mathbf{y}_s = [\mathbf{y}_R \ \cdots \ \mathbf{y}_1 \ \mathbf{y}_0 \ \mathbf{y}_{-1} \ \cdots \ \mathbf{y}_{-R}]^T,$$

equation (9) can be solved in two steps. Firstly, the vector \mathbf{y}_s^{i+1} should be calculated using the following equation:

$$\mathbf{L} \cdot \mathbf{y}_s^{i+1} = \mathbf{f}_s(\mathbf{x}_s^i) + \mathbf{d}_0 \cdot \mathbf{x}_s^i. \quad (11)$$

Next, vector \mathbf{x}_s^{i+1} should be determined using equation (10). The vector \mathbf{x}_s^{i+1} allows for beginning the next iteration. It should be noted that all of the operations described above use N-dimensional vectors only, and any inverse matrix should be calculated. This is a significant benefit of the proposed algorithm.

Two problems arise for the algorithm based on (9):

- Does it converge?
- How should the element d_0 be selected?

This paper presents examples to address the above questions.

3. Simplest application examples

A. Elementary convergence test.

An extremely simple case is considered to test the algorithm convergence. When the first derivative

$$dx/dt = \cos \Omega t \quad (12)$$

is known, one needs to solve for the $x(t)$ function. The respective finite-difference equations take the following form:

$$\mathbf{L} \cdot \mathbf{U} \cdot \mathbf{x}_s^{i+1} = \mathbf{f}_s + \mathbf{d}_0 \cdot \mathbf{x}_s^i \quad (13)$$

where: $\mathbf{x}_s = [\mathbf{x}_R \ \cdots \ \mathbf{x}_1 \ \mathbf{x}_0 \ \mathbf{x}_{-1} \ \cdots \ \mathbf{x}_{-R}]^T$

$$\mathbf{f}_s = [\mathbf{f}_R \ \cdots \ \mathbf{f}_1 \ 0 \ \mathbf{f}_{-1} \ \cdots \ \mathbf{f}_{-R}]^T$$

for $\mathbf{f}_r = \cos(r \cdot 2\pi / (2R + 1))$.

Convergence tests were conducted at $\Omega = 1,0$ [1/sec] and for $R = 25$ by solving equations (13) recurrently using procedures (10) and (11), starting from $x(t) = 0$. Figure 1a illustrates the waveform of function $x(t)$ obtained at $d_0 = 0,1 \cdot \Omega$, $d_0 = 1,0 \cdot \Omega$ and $d_0 = 10,0 \cdot \Omega$ for the selected iterations, while Fig. 1b illustrates the resulting amplitudes at the successive iterations.

The convergence is strongly dependent on the d_0 value. The function achieves the expected shape at $d_0 = 0,1 \cdot \Omega$ after only two iterations, excluding an arbitrary constant value. The test at $d_0 = 1,0 \cdot \Omega$ demonstrated that over 15 iterations are required, and the final waveform is achieved with damping oscillations. The algorithm converges very slowly at larger values of $d_0 = 0,1 \cdot \Omega$.

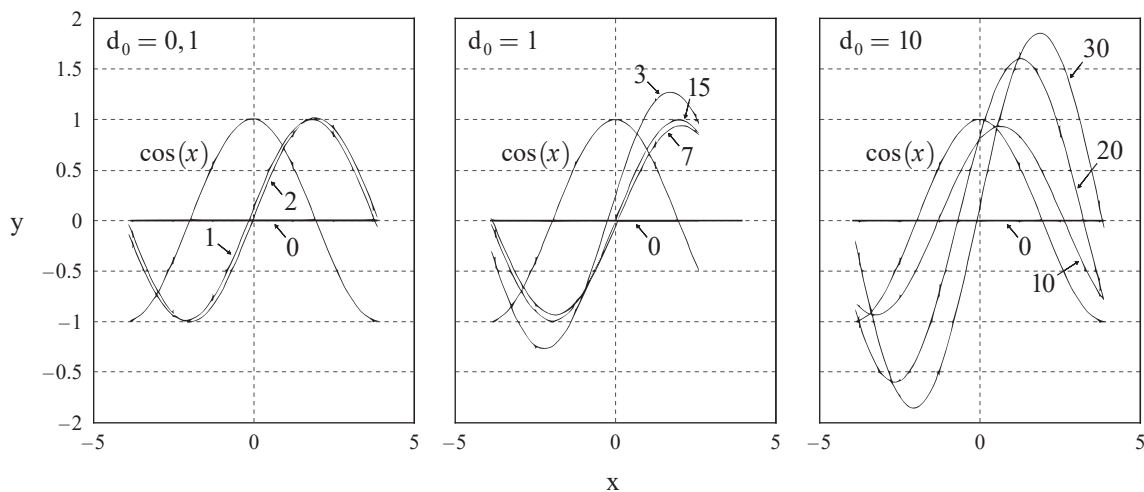


Fig. 1a. Wave-forms for selected iterations at $\Omega = 1,0$, $d_0 = 0,1$, $d_0 = 1,0$ and $d_0 = 10,0$

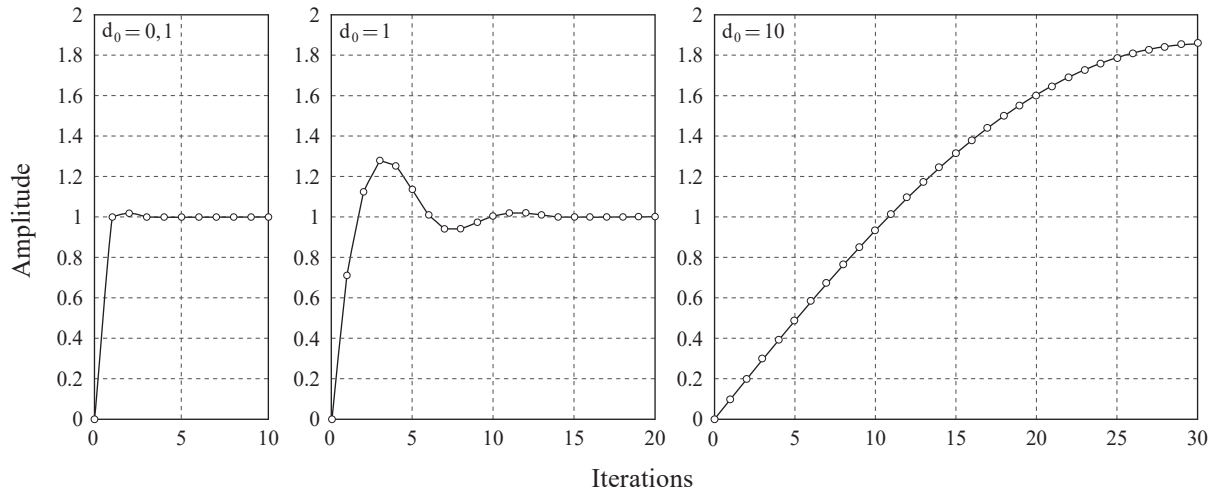


Fig. 1b Amplitudes for selected iterations at $\Omega = 1,0$, $d_0 = 0,1$, $d_0 = 1,0$ and $d_0 = 10,0$

B. Elementary circuit with nonlinear coil.

In [6], the steady-state solution for the elementary circuit in Fig. 2 was considered using the algorithm based on equation (5). Below, the analysis is repeated using the improved algorithm presented in this paper in order to demonstrate its advantages.

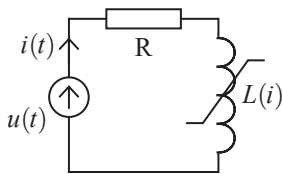


Fig. 2 Elementary circuit with nonlinear coil

The new algorithm requires the circuit equation to take the normal form, as follows

$$\frac{d}{dt} \psi = -R_L \cdot i + U_0 + U_m \cdot \cos \Omega t. \quad (14)$$

The nonlinear relation between the flux linkage and the current is assumed as

$$\psi(i) = L(i) \cdot i = \frac{L}{1 + b \cdot |i|} \cdot i. \quad (15)$$

The finite-difference equations determining the steady-state solution are as follows:

$$\mathbf{L} \cdot \mathbf{U} \cdot \Psi_s^{i+1} = -\mathbf{R}_L \cdot \mathbf{i}_s^i + \mathbf{u}_s + \mathbf{d}_0 \cdot \Psi_s^i, \quad (16)$$

where: $\Psi_s = [\Psi_R \ \dots \ \Psi_1 \ \Psi_0 \ \Psi_{-1} \ \dots \ \Psi_{-R}]^T$,
 $\mathbf{i}_s = [i_R \ \dots \ i_1 \ i_0 \ i_{-1} \ \dots \ i_{-R}]^T$,
 $\mathbf{u}_s = [u_R \ \dots \ u_1 \ u_0 \ u_{-1} \ \dots \ u_{-R}]^T$,
 $u_r = U_0 + U_m \cdot \cos(\Omega \cdot t_r)$,
 $t_r = r \cdot 2\pi / (\Omega \cdot (2R + 1))$.

Matrices \mathbf{L} and \mathbf{U} are calculated using any algorithm for \mathbf{LU} decomposition. The nonlinear relationship (15) is considered, assuming that

$$\psi_r^i = L(i_r^{i-1}) \cdot i_r^i \quad \text{for} \quad -R < r < R. \quad (17)$$

Two options for the algorithm based on equations (16) and (17) were developed and tested:

Algorithm 1 assumes that the vector \mathbf{i}_s^i in (16) is calculated at successive iterations, using the relationship

$$i_r^i = L(i_r^{i-1})^{-1} \cdot \psi_r^i. \quad (18)$$

Algorithm 2 has two iterative loops. The first loop try to satisfy relation $d_0 \cdot \Psi_s^{i+1} \approx d_0 \cdot \Psi_s^i$, assuming that the relation (15) is linear for fixed values i_r . The equation (16) is solved in this loop iteratively until $\Psi_s^{i+1} \approx \Psi_s^i$ at assumed accuracy. The second loop takes into account nonlinear relation (15). In the second loop, the equation (16) is solved iteratively again, starting from the results of the first loop. Now, values i_r and the parameters $L(i_r)$ are recalculated from (17) and (18) at each iteration, until $\Psi_s^{i+1} \approx \Psi_s^i$ at assumed accuracy.

Both algorithms were implemented in the MATLAB package. The first tests concentrated on the proper selection of the d_0 parameter. The following calculations were performed for the data: $R_L = 0,2$ [Ω], $L = 1,0$ [H], $U_0 = 0,0$ [V], $U_m = 1,0$ [V], $\Omega = 1,0$ [1/sec] and $b = 0,4$ [1/A], which are the same as those in [6]. Three values of d_0 were selected: $d_0 = 0,1 \cdot \Omega$, $d_0 = 1,0 \cdot \Omega$ and $d_0 = 10,0 \cdot \Omega$, which are the same as those for the convergence test described in the previous subchapter. During the period, 201 time instants were selected; that is, $R = 100$. The algorithm begins with the solution for the linear coil $L(i) = L$. It should be noted that, in these algorithms, operations with matrices are unnecessary, and all calculations can be performed with numbers only because equation (14) has only one dimension.

The results of the convergence test at $d_0 = 0,1 \cdot \Omega$ are illustrated in Figs. 2a and 2b.

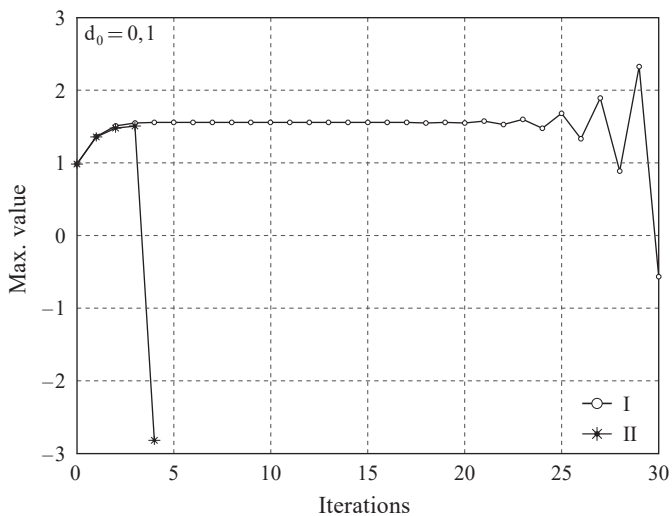


Fig. 2a Amplitude of current waveform for successive iterations at $\Omega = 1,0, d_0 = 0,1$; curve I – Algorithm 1, curve II – Algorithm 2

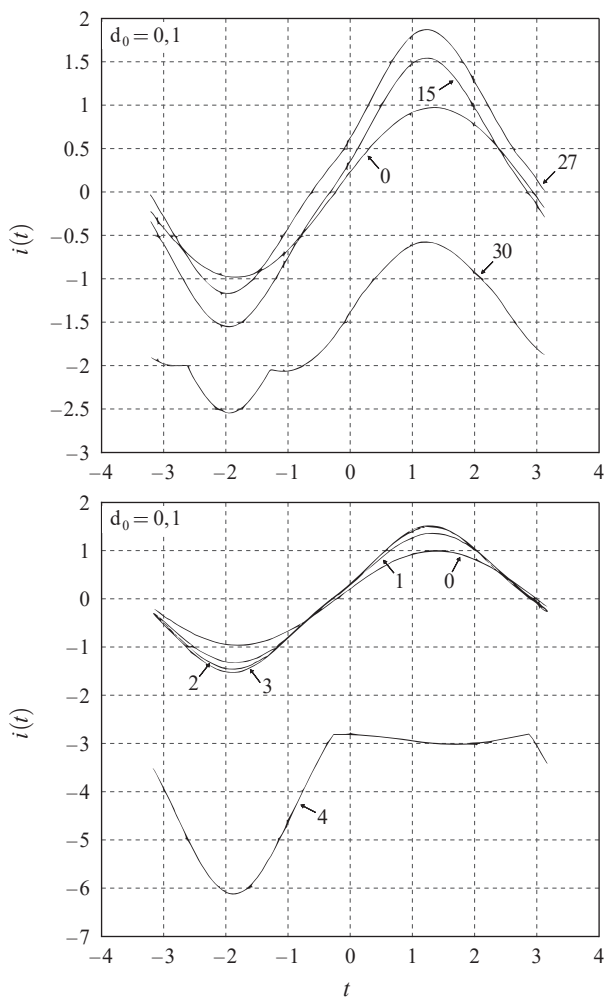


Fig. 2b Current wave-forms for selected iterations at $\Omega = 1,0, d_0 = 0,1$; left – Algorithm 1, right – Algorithm 2

These results indicate that both algorithms are unstable at $d_0 = 0,1 \cdot \Omega$. Algorithm 1 provides stable solutions after five iterations, but the long-term calculations are unstable. Algorithm 2 is unstable in several iterations. It can be concluded that the parameter d_0 should be determined for a given problem.

The results of the convergence tests at $d_0 = 1,0 \cdot \Omega$ and $d_0 = 10,0 \cdot \Omega$ are illustrated in Fig. 3. This figure presents the amplitudes of the current wave-forms in successive iterations for both algorithms. Algorithm 2 leads to a final result more rapidly, and at $d_0 = 1,0 \cdot \Omega$, only a few iterations are required. So, Algorithm 2, at $d_0 = 1,0 \cdot \Omega$, is recommended for further calculations in this case.

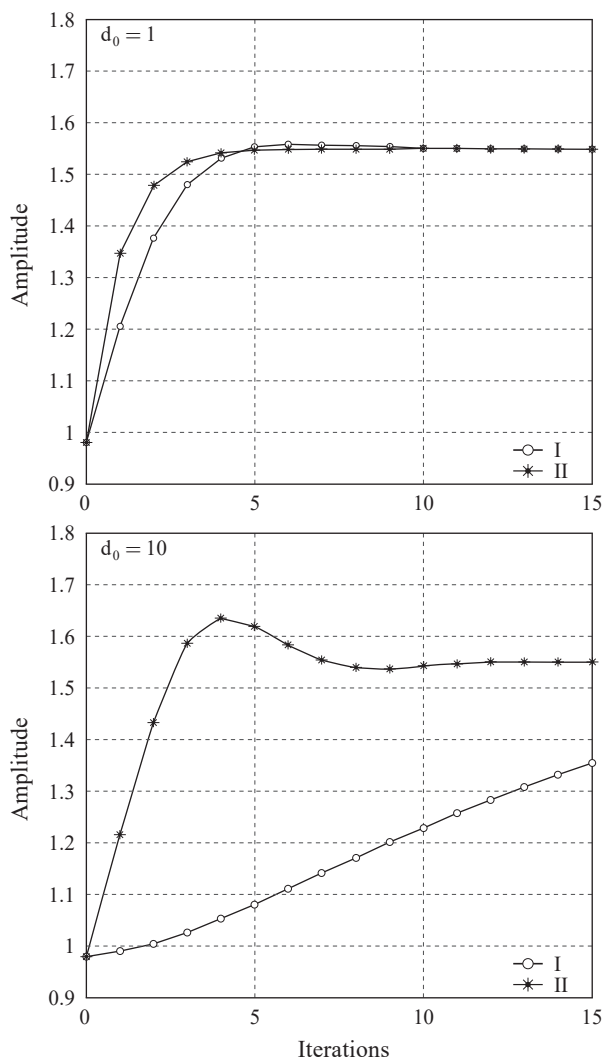


Fig. 3 Amplitude of current wave-forms for successive iterations at $\Omega = 1,0, d_0 = 1,0$ and $d_0 = 10,0$; curve I – Algorithm 1, curve II – Algorithm 2

Figure 4 illustrates the current wave-forms in successive iterations obtained at $d_0 = 1,0$ using both algorithms. The final curves in Fig. 4 precisely replicate those presented in [6] for the same exemplary case.

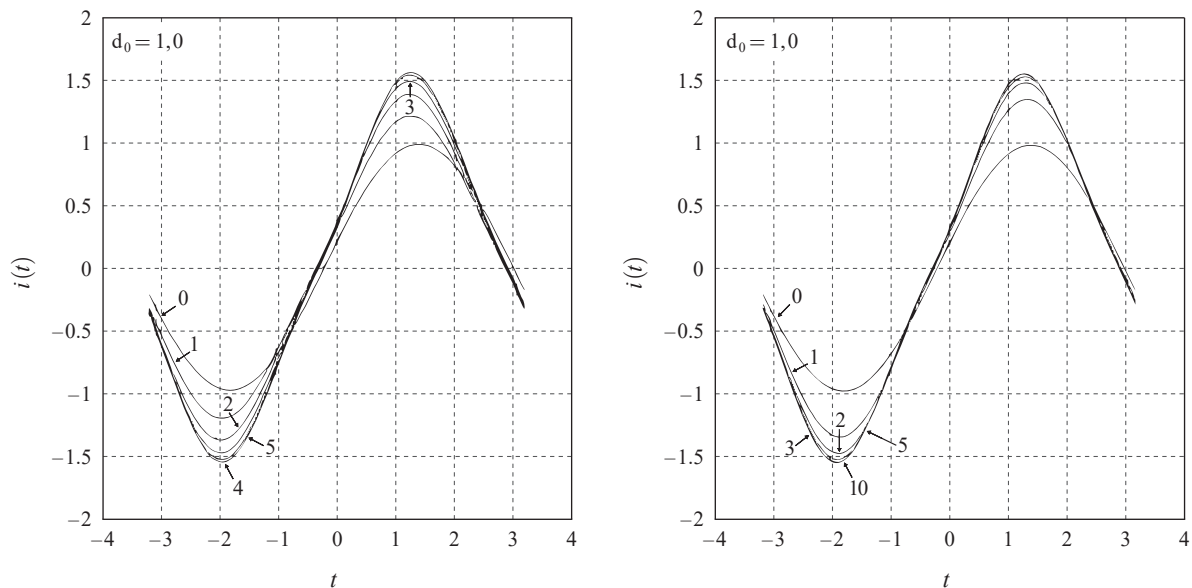


Fig. 4 Current wave-forms for successive iterations at $\Omega = 1,0$, $d_0 = 1,0$ curve I – Algorithm 1, curve II – Algorithm 2

The current wave-forms were calculated for three voltages: 1,0 [V], 1,2 [V] and 2,0 [V], to test the algorithm sensitivity with respect to the coil nonlinearity. The final wave-forms are presented in Fig. 5, and are identical to those presented in [6].

Figure 6 illustrates an influence of the DC component in voltages on the current waveform. The current wave-forms deform as expected, and the exact same current wave-forms as in Figs. 5 and 6 have been achieved by the simulations.

The test results for the elementary circuit with a nonlinear coil confirm that the algorithm described in this paper can be effectively applied to determining a periodic steady-state solution to nonlinear equations of electromagnetic devices, omitting the problem of high dimensions.

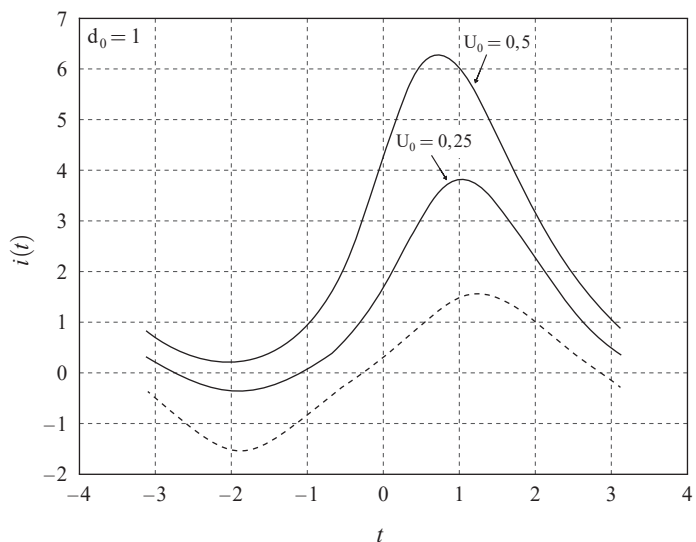


Fig. 6 Final current wave-forms at $U_m = 1,0$ [V], $U_0 = 0,25$ [V] and $U_0 = 0,5$ [V]

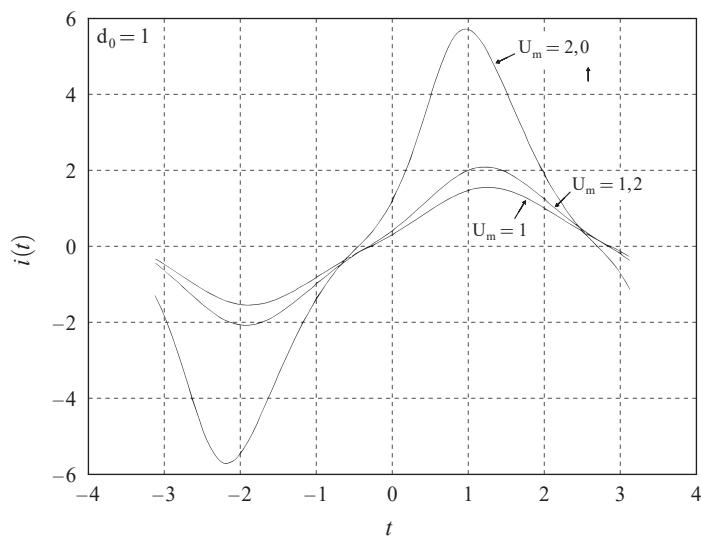


Fig. 5 Final current wave-forms for $U_0 = 0,0$ [V], $U_m = 1,0$ [V], $U_m = 1,2$ [V] and $U_m = 2,0$ [V]

4. Conclusions

The paper presents a new means of integrating nonlinear differential equations in determining periodic steady states directly in the time domain. The discrete differential operator forms the basis for the difference equations that determine the required solution. These nonlinear equations are modified to omit difficulties when seeking a numerical solution. Moreover, LU decomposition is used to reduce the numerical computation complexity. As a result, the mathematical operations are reduced to matrices with dimensionalities of the differential

equations, being independent of the number of time instants over the period.

Acknowledgements. This research has been carried on in the frame of project E-2/581/2016/DS funded by The Polish Ministry of Science and Higher Education.

REFERENCES

- [1] T. Hara, T. Naito and J. Umoto, "Time-periodic finite element method for nonlinear diffusions equations", *IEEE Trans. Magn.*, 21(6), 2261–2264 (1985).
- [2] O. Biro and K. Preis, "An efficient time domain method for nonlinear periodic eddy current problems", *IEEE Trans. Magn.*, 42(4), 695–698 (2006).
- [3] N. Garcia, "Periodic steady-state solutions of nonlinear circuits based on a differentiation matrix", *Proc. of 2010 IEEE Int. l Symp. Circuits and Systems*, 141–144 (2010).
- [4] T.J. Sobczyk and M. Radzik, "Direct determination of periodic solution in time domain for electromechanical converters", *Technical Transactions – Electrical Eng.*, Cracow Univ. of Tech., 112(2-E), 73–82 (2015).
- [5] M. Radzik and T.J. Sobczyk, "An algorithm of time domain steady-state analysis for electrical machines accounting for saturation", *Proc. of SME 2017, IEEE Explore* (978–1–5386–0359–8/17/\$31.00 ©2017 European Union), Paper 13, (2017).
- [6] T.J. Sobczyk and M. Radzik, "A new approach to steady state analysis of nonlinear electrical circuits", *COMPEL*, Emerald Pub. Ltd., 36(3), 716–728 (2017).
- [7] T.J. Sobczyk and M. Radzik, "Application of novel discrete differential operator of periodic function to study electromechanical interaction", *Bull. Pol. Ac.: Tech.* (66)5, 645–653 (2018).
- [8] S. Yamada, K. Besho, and J. Lu, "Harmonic balance finite element method application for nonlinear magnetic analysis", *IEEE Trans. Magn.*, Vol. 25, 2971–2973 (1989).
- [9] A. Semlyen, E. Acha, and H.W. Dommel, "Newton-type algorithms for the harmonic phasor analysis of nonlinear power circuits in periodical steady state with special reference to magnetic nonlinearities", *IEEE Trans. Power Delivery*, Vol. 6, 1090–1098 (1991).
- [10] T.J. Sobczyk, "Direct determination of two-periodic solution for nonlinear dynamic systems", *COMPEL*, James & James Science Pub. Ltd., Vol. 13, 509–529 (1994).
- [11] J. Gyselinck, P. Dular, C. Geuzaine, and W. Legros, "Harmonic-balance finite element modeling of electromagnetic devices: a novel approach", *IEEE Trans Magnetics*. 38(2), 521–524 (2002).
- [12] O. Deblecker and J. Lobry, "A new efficient technique for harmonic-balance finite element analysis of saturated electromagnetic devices", *IEEE Trans. Magn.*, Vol. 38, 535–538, (2006).
- [13] X. Zhao, L. Li, J. Lu, Z. Cheng, and T. Lu, "Analysis of the saturated electromagnetic devices under CD bias condition by the decomposed harmonic balance method", *COMPEL*, Vol. 3, 498–513 (2012).
- [14] E. Lelarsmee, A.E. Ruchli, and A. Sangiovanni-Vincentelli, "The waveform relaxation method for time-domain analysis of large scale integrated circuits", *IEEE Trans. CADIC* 1(3), 131–145 (1982).
- [15] G. Caron, T. Henneron, F. Piriou, and J-C Mipo, "Time-periodic condition of nonlinear magnetostatic problem coupled with electric circuit imposed by waveform relaxation method", *IEEE Trans. Magnetics* 52(3) (2016).
- [16] G. Caron, T. Henneron, F. Piriou, and J-C Mipo, "Waveform relaxation-Newton method to determine steady state operation: application to three-phase transformer", *COMPEL* 36(3), 729–740 (2017).